HHS Public Access

Author manuscript

Radiol Infect Dis. Author manuscript; available in PMC 2019 November 05.

Published in final edited form as:

Radiol Infect Dis. 2018 March ; 5(1): 7–13. doi:10.1016/j.jrid.2018.01.002.

PET and CT features differentiating infectious/inflammatory from malignant mediastinal lymphadenopathy: A correlated study with endobronchial ultrasound-guided transbronchial needle aspiration

Haiyan Wang[a], **Qing Kay Li**[b], **Martin Auster**[c], **Gary Gong**[d,*]

[a]Shandong Medical Imaging Research Institute, Shandong University, Jingwu Road No.324, Jinan, Shandong 250021, China

[b]Department of Pathology, The Johns Hopkins University Bayview Medical Center, 4940 Eastern Avenue, Baltimore, MD 21224-2780, USA

[c]Imaging Department, The Johns Hopkins University Bayview Medical Center, 4940 Eastern Avenue, Baltimore, MD 21224-2780, USA

[d]Department of Radiology & Radiological Sciences, The Johns Hopkins University Hospital, Phipps B-125, 600 North Wolfe Street, Baltimore, MD 21287, USA

Abstract

Purpose: To explore the advantages of differentiating inflammatory from malignant thoracic lymph nodes by integrating their features on positron emission tomography (PET) and computed tomography (CT).

Material and method: Following institutional review board approval, PET and CT parameters of thoracic lymph nodes were examined based on their pathologic diagnosis via endobronchial ultrasound-guided transbronchial needle aspiration. The standardized uptake value (SUV) of PET and CT findings of the long- and short-axis diameters, axial short to long diameter ratios (S/L), and measured nodal CT values of the lymph nodes were compared and analyzed statistically.

Results: A total of 124 lymph nodes from 70 patients were studied. The inflammatory and malignant lymph nodes differed significantly in their SUV ($P = 0.008$), short-axis diameters (SAD, $p < 0.001$), long-axis diameters (LAD, $p = 0.002$) and S/L ratios ($p < 0.001$). They did not differ significantly in non-contrast enhanced CT values ($p = 0.304$). The sensitivities, specificities, positive predictive values, negative predictive values, diagnostic accuracies and diagnostic odds ratios (DOR) were: 1) elevated SUV alone - 95.31% (61/64), 20% (12/60), 55.96% (61/109), 80% (12/15), 58.87% (73/124), and 5; 2) combined SUV + SAD - 89.06%, 53.33%, 67.06%, 82.05%, 71.77%, and 9.31; 3) combined SUV + S/L ratio - 87.5%, 93.33%, 93.33%, 87.5%, 90.32%, and 98, respectively.

*Corresponding author. Fax: +410 614 1213. ggong1@jhmi.edu (G. Gong).

Peer review under responsibility of Beijing You'an Hospital affiliated to Capital Medical University.

Conclusion: Increased SUV, SAD, LAD, and S/L ratio are accurate PET/CT parameters to characterize inflammatory or malignant lymph nodes. SUV has high sensitivity but low specificity, low positive and negative predictive values, and low DOR. The SUV + SAD and SUV + S/L ratios have higher specificity, positive and negative predictive values, diagnostic accuracy and DOR.

Keywords

PET/CT; Positron emission tomography; Computed tomography; Mediastinal lymph nodes; EBUS

1. Introduction

Enlarged thoracic (hilar and mediastinal) lymph nodes are common clinical scenarios. Lymph nodes may be enlarged due to benign causes such as inflammation or infection, or due to malignancy especially metastatic lymphadenopathy. It is crucial to differentiate inflammatory from malignant lymph node under many clinical situations. For example, the nodal status can dictate the course of therapy and prognosis of lung cancer. Although CT has been widely used for the preoperative evaluation of tumor size and adjacent structural details, numerous studies have shown the limited reliability of CT in lymph node staging [1,2]. CT diagnostic criteria using an upper limit of 1.0 cm or more for malignancy can overlook early or partial malignant infiltration of the node, and a number of reviews and meta-analyses have shown this limited reliability of CT in lymph node staging [3]. 18F-Fluorodeoxy glucose positron emission tomography−computed tomography (18F-FDG-PET) can detect malignant lymph nodes of even normal size, thus overcoming one of the major limitations of CT. However the diagnostic value of PET has also been reduced by its low spatial resolution. Infection or inflammation can also cause high FDG uptake leading to false positivity [4]. Integrated PET and CT (PET/CT) had been found to outperform CT or PET alone as it provides structural and functional information of disease status at the same time [5] although tissue diagnosis remains the gold standard.

Endobronchial ultrasound (EBUS)-guided transbronchial needle aspiration (TBNA) is a proven accurate technique for histological diagnosis of thoracic lymph nodes [6]. However, this procedure is invasive in nature, which cannot be performed on patients who have other comorbidities. There is no single non-invasive imaging method that was fairly conclusive in evaluating potential chest nodal involvement in otherwise operable lung cancer patient under routine clinical conditions [7].

The aim of this study was to retrospectively analyze the different PET and CT features of suspicious thoracic lymph nodes sampled by EBUS-TBNA and to explore the advantages of combining the most predictive parameters of PET and CT to derive better diagnostic parameters in differentiating inflammatory from malignant thoracic lymph nodes.

2. Materials and methods

2.1. Patients

Following institutional research and ethical review board approval and HIPAA compliance, a total of 70 consecutive patients with hilar and mediastinal lymphadenopathy detected on

chest CT were enrolled in the study. There were 39 males and 31 females with mean age of 62.45 ± 14 years (range 20–93years). The radiological and pathological data of those 70 patients who underwent both PET/CT exams and EBUS-TBNA procedures for hilar and mediastinal lymph nodes sampling were retrospectively analyzed.

2.2. PET/CT

All PET/CT studies were acquired in the same PET center using a combined in-line PET/CT system (Discovery RX; GE Healthcare, USA), within 3 weeks from the EBUS-TBNA.

Patients fasted for at least 6 h before the exam; the scanning was performed 60 min after IV administration of 18F-FDG (4.5e5.5 MBq/kg). Scanning was performed from the base of the skull to the pelvis with patients in supine position. To obtain a precise anatomic correlation between PET and CT images, scanning was performed with the arms in the overhead position for both PET and CT. Coronal and transverse data sets were reconstructed. Diagnostic non-contrast-enhanced CT was initially performed at 120 KV and with automatic current adjustment (maximum, 300 mA) according to the patient's weight. The axial CT images (in 5 mm thickness) were reconstructed using B30f kernel for mediastinal algorithm. Images were transferred to PACS workstations for detailed analysis. Nuclear medicine board certified specialists from nuclear medicine department interpreted the PET images while the CT images were interpreted by board certified radiologists. Abnormal 18F-FDG uptake was defined as accumulation outside the normal anatomic structures and of greater intensity than background activity inside the normal structures. Any abnormally elevated visual focus of 18F-FDG uptake over that of the background was deemed to represent tumor tissue. The uptake of the radiotracer was also assessed semi-quantitatively using the standardized uptake value (SUV) method.

According to the result of most authors [7,8], hilar and/or mediastinal lymph nodes were considered positive for malignant if they showed increased FDG uptake (SUV thresholds: SUV >2.5). CT images were evaluated in respects of LADs and SADs of the lymph nodes, their axial S/L ratios, nodal locations and average CT HUs (Hounsfield unit). A currently accepted upper limit of SAD >1.0 cm [9] was used for malignancy positivity. According to our previous study, the axial S/L ratio >0.7 was the most accurate positive predictor for malignancy.

2.3. EBUS-TBNA

After PET/CT and/or CT identification of the lymph nodes in question, their locations were correlated by EDUS through a bronchofibervideoscope (Olympus Exera). Subsequent cytological specimens were collected via EBUD-TBNA with 22-gauge needle, and core biopsies were obtained using 19-gause needle. On-site evaluation of biopsy sample adequacy was performed by an experienced cytotechnologist. In many patients, multiple passes were performed to ensure sample adequacy. Core-biopsy samples were sent for frozen-section with final pathology diagnosis made at our institution. When malignant tumor cells were confirmed, the sampled nodes were labeled as positive for malignancy or metastatic nodes. Inflammatory/infectious lymphadenopathy were diagnosed with characteristic histology findings without the presence of tumor cells. If neither malignant cell no inflammatory

changes were found in lymph node sampling, the specimens were labeled as non-diagnostic and the data were excluded. None-enlarged lymph nodes were not sampled and were not included in this study. Some lymph node levels are difficult for EBUS to gain access, such as paraesophagaeal nodes or aortopulmonary window nodes which are also excluded from this study.

3. Statistical analysis

Data analysis was performed using SPSS statistical software (IBM SPSS Statistics 20; Chicago, IL, USA). Continuous variables were analyzed using one-way ANOVA, and dichotomous variables were analyzed with Mann–Whitney U test. Findings on integrated PET-CT were compared with that of pathological result of EBUS-TNBA in order to determine their diagnostic sensitivity [TP/(TP + FN)], specificity [TN/ (TN + FP)], positive predictive value [PPV, TP/(TP + FP)], negative predictive value [NPV, TN/(TN + FN)], diagnostic accuracy [(TP + TN)/n], and DOR [(TN × TP)/(FP × FN)] [10]. All reported p-values were two-sided, and a p-value of <0.05 was considered statistically significant.

4. Result

From our 70 subjects, there were 124 lymph nodes studied by PET/CT with subsequent pathologic correlation. The locations of the lymph nodes sampled by EBUS-TBNA were summarized in Table 1, which were determined according to the lung cancer lymph node map proposed by the International Association for the Study of Lung Cancer (IASLC). The most frequently sampled nodes were 4R (40/124, 32.26%) and 7 (27/124, 21.77%).

The overall histological diagnoses of all 124 lymph nodes were summarized in Table 2. Among them, 64 lymph nodes were malignant and 60 were inflammatory lymph nodes. The LAD and SAD of inflammatory lymph nodes (Mean ± SD) were 1.87 ± 0.64 cm and 1.07 ± 0.38 cm, respectively. However, the LAD and SAD of malignant lymph nodes (Mean ± SD) were 2.38 ± 1.11 cm and 2.03 ± 1.01 cm, respectively. Both the LAD ($p = 0.002$) and SAD ($p < 0.001$) of malignant lymph nodes were significantly greater than that of inflammatory lymph nodes. Notice that the mean SAD of benign nodes is slightly greater than 1 cm in this study. The axial S/L ratio of inflammatory lymph nodes was 0.57 ± 0.09 and the axial S/L ratio of malignant lymph nodes was 0.85 ± 0.11. This differences of axial S/L ratio is significant between inflammatory versus malignant nodes ($p < 0.001$). The mean CT HU (Mean ± SD) of the lymph nodes on non-contrast enhanced scans were 33.07 ± 14.31 HU for inflammatory and 35.41 ± 9.78 HU for malignant nodes, respectively, without statistical difference ($p = 0.304$). Those detailed PET/CT numerical variables were summarized in Table 3. The SUV, as expected, differed significantly ($P = 0.008$) between inflammatory and malignant groups. We further combined those data with multivariate analysis to extract the parameters with best diagnostic values especially the results of combining SUV>2.5 with SAD >1.0 cm (SUV + SAD) and combining SUV>2.5 with axial S/L ratio > 0.7 (SUV + SLR). These results were summarized in Table 4.

5. Discussion

Numerous studies, primarily using CT and PET to characterize the nature of mediastinal lymph nodes, have been conducted due to its clinical importance in determining treatment options, monitoring treatment responses, and determining prognosis. Those results have greatly improved our knowledge in this regards and benefited our patients significantly. For example, there is no difficulty in diagnosing nodes with markedly abnormal features, i.e., large nodes with necrosis or extra-capsular invasion on CT or nodes with markedly elevated SUV on PET. However, accurate identification of suspicious or borderline thoracic lymph nodes remains a challenge in our clinical practice when facing a patient with malignancy in the chest or elsewhere. It is with this challenge in mind we studied a group of patient who presented with questionable chest lymph nodes in mediastinum and/or hilum by examining their imaging features on CT and PET as correlated with their pathological diagnosis by EBUS-TBNA for each individual nodes.

Both CT and MRI can provide good structural details in size, contour, border sharpness, signal or density character, and tissue components such as calcification, fat, or fluid. When a lymph node does not have those readily identifiable features, its size is usually used as a discriminating factor and the widely accepted criteria of SAD greater than 1 cm for malignancy has been used [7,9,10]. In our study, both the mean LAD (1.87 ± 0.64 cm) and SAD (1.07 ± 0.38 cm) in malignant nodes are significantly greater than that of inflammatory nodes. However, decision based on large size alone can overlook early metastatic nodes that had not been significantly enlarged by the malignancy [11]. Further more, even enlarged nodes could still be benign. This has been clearly demonstrated on this study, as well as by numerous reports. Therefore we examined the axial S/L ratio of the nodes in detail. The axial S/L ratio of malignant lymph nodes (0.85 ± 0.11) was significantly ($p < 0.001$) greater than that of inflammatory lymph nodes (0.57 ± 0.09). Of note, similar results that rounded appearing nodes are more likely to represent metastatic nodes in the neck region have been long recognized on CT and MRI [12].

Unlike CT or MRI, PET images biochemical or physiologic phenomena [8,11] in living tissue. PET has shown substantial benefits during the past decade in helping with noninvasive diagnosis and preoperative staging of lung and extra-thoracic cancers [13]. Malignant tissues usually present with significantly increased SUV, which is the single most valuable strength of PET, due to their higher metabolic rate. PET is superior to CT in mediastinal and hilar lymph node staging with increased sensitivity but decreased specificity in lung cancer patients [14]. The sensitivity of PET in our study was very high (95.31%) with a low specificity (20%), possibly from sample population bias. Inflammatory/ granulomatous processes (such as tuberculosis, histoplasmosis, aspergillosis, coccidiomycosis, sarcoidosis, Wegener's granulomatosis, and even pneumonia) can produce false-positive results, especially in cases of a fulminate process [15]. We observed a 38.7% (48/ 124) false positivity of PET when using SUV (>2.5) alone as the diagnostic criteria, comparable to literatures when the SUV is adjusted. Similarly, neoplasms with lower metabolic activity, such as bronchoalveolar cell carcinoma and carcinoid, can sometimes give a borderline or a false-negative result [16,17]. False-negative results can also be caused by PET technique itself [18], for example, FDG tumor uptake can be competitively inhibited

by blood glucose in patients with high blood glucose levels (>250 mg/dL) during the study. Additionally, PET has a low spatial resolution, resulting in false-negative results in lesions <7 mm in size or even up to 1 cm [19,20]. The false negative rate was 4.1% (3/73) in our series when using SUV (>2.5) was used as a single diagnostic criteria.

Given the high sensitivity of PET and CT morphologic characteristics of those nodes, it is only logical to combine physiologic and anatomic imaging features together to develop a synergistic paradigm to achieve higher diagnostic accuracy. When using SUV + SAD as diagnostic criteria, better results were achieved with the specificity of 53.33%, PPV of 67.06%, NPV of 82.05%, and diagnostic accuracy at 71.77. SUV + S/L ratio as diagnostic criteria yielded a slightly lower sensitivity (87.5%) than using SUV alone, but the specificity (93.33%), PPV (93.33%), NPV (87.5%) and accuracy (90.32%) were all significant improved. It is worth noting that currently, the PET/CT scans are read separately by diagnostic radiologists and nuclear medicine physicians in slightly more than half of the institutions (based on personal survey). After the PET/CT was performed, the PET and CT images were sent separately to PET and CT sections and the 2 groups of readers used their own established modality-specific diagnostic criteria in minds to finalize their reports. It seemed that one could achieve a better diagnostic accuracy by combining the individual features of PET and CT to a single decision making point, as supported by our results.

The DOR of a test obtained with different combinations of sensitivity and specificity may be used as a single summary measure, and it is the ratio of the odds of positivity in diseased relative to the odds of positivity in the non-diseased conditions [21]. The value of a DOR ranges from 0 to infinity, and the higher it is, the better it discriminates test performance. A value of 1 indicates that a test does not discriminate between patients with the disorder from those without it. Values lower than 1 point to more false negative tests among the diseased. In our study, we have found that both the combined SUV + SAD (DOR = 9.31) and combined SUV + S/L ratio (DOR = 98) have higher DORs than that of SUV alone (DOR = 5), indicating that combined PET and CT criteria seemed to be advantageous in diagnostic accuracy for identifying malignant lymph nodes from inflammatory lymph nodes. We therefore proposed such a combined diagnosis criteria in this study. Using SUV + SAD or SUV + S/L ratio of CT could have significantly reduced the numbers of false positive lymph nodes (from 48 to 28 and from 48 to 4) (Fig. 1). The low-grade lymphomas presented with large-size nodes but lower SUV and small sized malignant nodes (likely below PET detection threshold) in our series contributed to the false negative findings on PET scan [16e18]. When those nodes were examined separately using individual PET or CT criteria alone, it was difficult to make the correct diagnosis. However, the combined larger size and high S/L ratio of those false negative node should have alerted the readers to perhaps call them as positive for malignancy despite their low SUV on PET, had the readers was using the combined diagnostic criteria as described in this study (Fig. 2). Nevertheless, this can only be tested in future prospective study. This study seemed to conclude that combining individual diagnostic criteria of CT and PET together when interpreting PET/CT exams outperformed using them separately in differentiating benign from malignant chest lymph nodes (see Figs. 3 and 4).

There are limitations to this study. The major limitation is its retrospective nature. Secondly, the patient selection is not blinded to prior imaging or clinical data. Patients enrolled for the study already presented with prior imaging recommendations for further evaluation of those nodes, which could produce bias error from the PET/CT interpretation, although this error could be either positive or negative statistically. This can also be addressed by future prospective study. Lastly, some lymph node stations are difficult to gain access by EBUS, such as the paraesophagaeal (level eight) nodes or aortopulmonary window (level five) nodes [22], which were excluded in this study. Additional correlative study of all the resected nodes in patients who underwent thoracotomy would provide more comprehensive results.

6. Conclusion

Thoracic nodal PET-SUV, SAD, LAD and axial S/L ratio on CT were accurate parameters to identify inflammatory or malignant lymph nodes. Increased SUV on PET had high sensitivity but low specificity thus lower diagnostic accuracy and DOR. Criteria using combined SUV + SAD or combined SUV + S/L ratio had higher specificities, positive and negative predictive values, diagnostic accuracies and DORs. Given the current paradigm of reading PET/CT exam separately by nuclear medicine physician and diagnostic radiologist in many institutions, we would propose that when making differential diagnosis of indeterminate chest lymph nodes on PET/CT exam, the combined criteria of nodal SAD and S/L ratio on CT and SUV on PET should be used to achieve better diagnostic accuracy. This approach deserves further prospective study to increase its strength.

References

[1]. McLoud TC, Bourgouin PM, Greenberg RW. Bronchogenic carcinoma: analysis of staging in the mediastinum with CT by correlative lymph node mapping and sampling. Radiology 1992;182:319–23. [PubMed: 1732943]

[2]. Scott WJ, Gobar LS, Terry JD, Dewan NA, Sunderland JJ. Mediastinal lymph node staging of non-small-cell lung cancer: a prospective comparison of computed tomography and positron emission tomography. J Thorac Cardiovasc Surg 1996;11:642–8.

[3]. Gross BH, Glazer GM, Orringer MB, Spizarny DL, Flint A. Bronchogenic carcinoma metastatic to normal-sized lymph nodes: frequency and significance. Radiology 1988;166:71–4. [PubMed: 3336704]

[4]. Ugurluer G, Kibar M, Yavuz S, Kuzucu A, Serin M. False positive 18F-FDG uptake in mediastinal lymph nodes detected with positron emission tomography in breast cancer: a case report. Case Rep Med 2013;2013: 459753. [PubMed: 23533427]

[5]. Liu Q, Peng ZM, Liu QW. The role of 11C-choline positron emission tomography-computed tomography and videomediastinoscopy in the evaluation of diseases of middle mediastinum. Chin Med J 2006;119: 634–9. [PubMed: 16635407]

[6]. Herth FJ, Krasnik M, Kahn N, Eberhardt R, Ernst A. Combined endoscopicendobronchial ultrasound-guided fine-needle aspiration of mediastinal lymph nodes through a single bronchoscope in 150 patients with suspected lung cancer. Chest 2010;138:790–4. [PubMed: 20154073]

[7]. Fritscher-Ravens A, Bohuslavizki KH, Brandt L. Mediastinal lymph node involvement in potentially resectable lung cancer: comparison of CT, positron emission tomography, and endoscopic ultrasonography with and without fine-needle aspiration. Chest 2003;123(2):442–51. [PubMed: 12576364]

[8]. Weber WA. Use of PET for monitoring cancer therapy and for predicting outcome. J Nucl Med 2005;46:983–95. [PubMed: 15937310]

[9]. Webb WR, Gatsonis C, Zerhouni EA. CT and MR imaging in staging non-small cell bronchogenic carcinoma: report of the Radiology Diagnosis Oncology Group. Radiology 1991;178:705–13. [PubMed: 1847239]

[10]. Will O, Purkayastha S, Chan C. Diagnostic precision of nanoparticle-enhanced MRI for lymph-node metastases: a meta-analysis. Lancet Oncol 2006;7:52–60. [PubMed: 16389184]

[11]. Kumar A, Dutta R, Kannan U, Kumar R, Khilnani GC, Gupta SD. Evaluation of mediastinal lymph nodes using F-FDG PET-CT scan and its histopathologic correlation. Ann Thorac Med 2011 1;6(1). 11–6. [PubMed: 21264165]

[12]. Steinkamp HJ, Cornehl M, Hosten N, Pegios W, Vogl T, Felix R. Cervical lymphadenopathy: ratio of long- to short-axis diameter as a predictor of malignancy. Br J Radiol 1995;68(807):266–70. [PubMed: 7735765]

[13]. Graeter TP, Hellwig D, Hoffmann K, Ukena D, Kirsch CM, Schäfers HJ. Medi- astinal lymph node staging in suspected lung cancer: comparison of positron emission tomography with F-18-fluorodeoxyglucose and mediastinoscopy. Ann Thorac Surg 2003;75:231–5. [PubMed: 12537221]

[14]. Gould MK, Kuschner WG, Rydzak CE. Test performance of positron emission tomography and computed tomography for mediastinal staging in patients with non-small-cell lung cancer: a meta-analysis. Ann Intern Med 2003;139(11):879–92 (2). [PubMed: 14644890]

[15]. Konishi J, Yamazaki K, Tsukamoto E. Mediastinal lymph node staging by FDG-PET in patients with non-small cell lung cancer: analysis of false-positive FDG-PET findings. Respiration 2003;70(5):500–6. [PubMed: 14665776]

[16]. Trukington TG, Coleman RE. Clinical oncologic PET: an introduction. Semin Roentgenol 2002;37:102–9. [PubMed: 12134363]

[17]. Chang JM, Lee HJ, Goo JM. False positive and false negative FDG-PET scans in various thoracic diseases. Korean J Radiol 2006;7(1):57–69. [PubMed: 16549957]

[18]. Goo JM, Im JG, Do KH. Pulmonary tuberculoma evaluated by means of FDG PET: findings in 10 cases. Radiology 2000;216:117–21. [PubMed: 10887236]

[19]. Kostakoglu L, Agress H, Goldsmith SJ. Clinical role of FDG PET in evaluation of cancer patients. Radio Graphics 2003;23:315–40.

[20]. Kim BT, Lee KS, Shim SS. Stage T1 non-small cell lung cancer: preoperative mediastinal nodal staging with integrated FDG PET/CT-a prospective study. Radiology 2006;241:501–9. [PubMed: 16966480]

[21]. Lv YL, Yuan DM, Wang K. Diagnostic performance of integrated positron emission tomography/computed tomography for mediastinal lymph node staging in non-small cell lung cancer: a bivariate systematic review and meta-analysis. J Thorac Oncol 2011;6:1350–8. [PubMed: 21642874]

[22]. Ohnishi R, Yasuda I, Kato T. Combined endobronchial and endoscopic ultrasound-guided fine needle aspiration for mediastinal nodal staging of lung cancer. Endoscopy 2011;43:1082–108. [PubMed: 21971924]

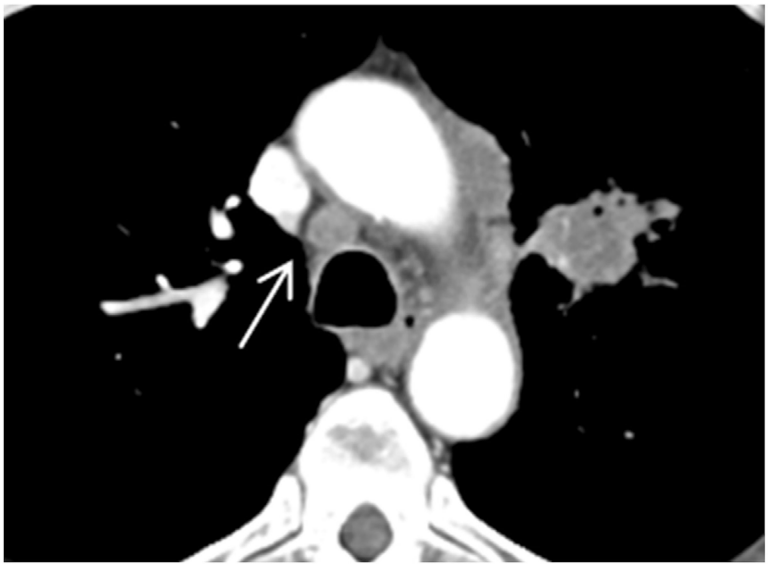

Fig. 1.

Axial CT image revealed a rounded lymph node on 4R (arrow). Long-axis diameter is 1.13 cm, and short-axis diameter is 0.97 cm. Axial S/L ratio is 0.86. The pathology result is non-small cell lung cancer.

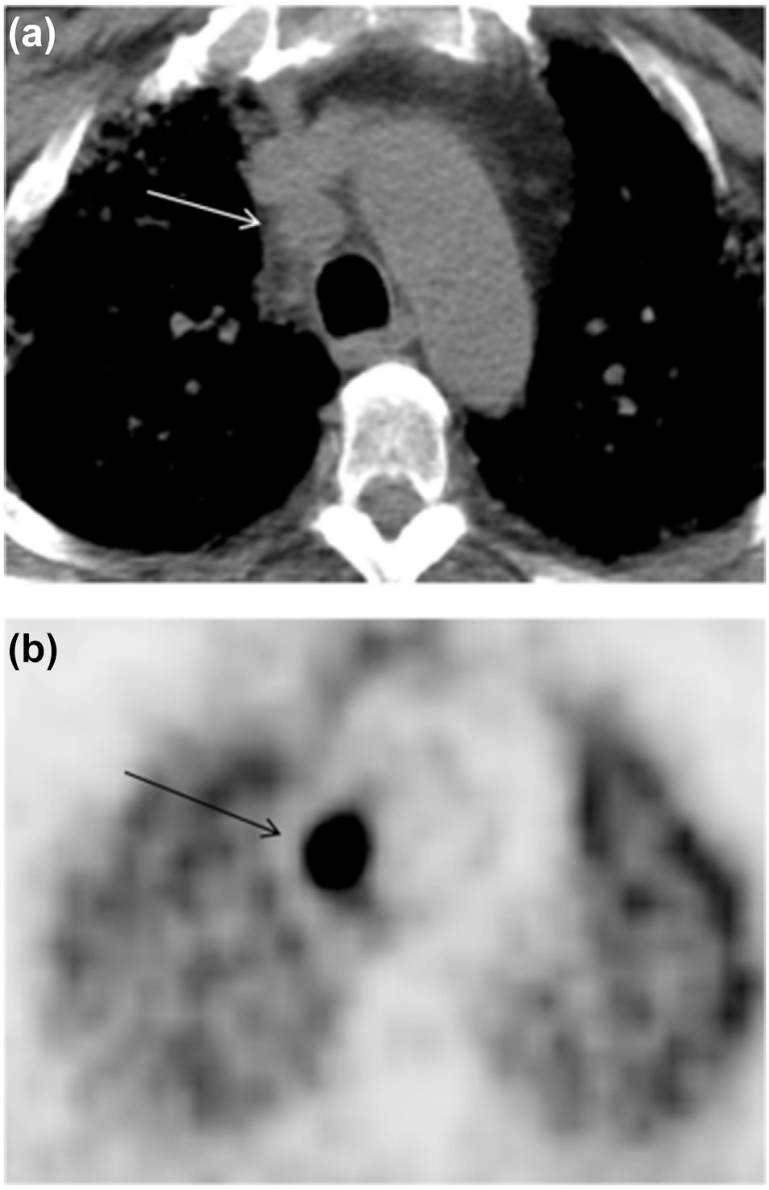

Fig. 2.

Axial CT image (a) revealed a rounded lymph node on 4R (arrow). Long-axis diameter is 1.86 cm, and short-axis diameter is 1.63 cm. The axial S/L ratio is 0.88. The lymph node has un-sharpness of border. The PET image (b) revealed high FDG uptake (arrow) of lymph node. The pathology result is squamous cell carcinoma.

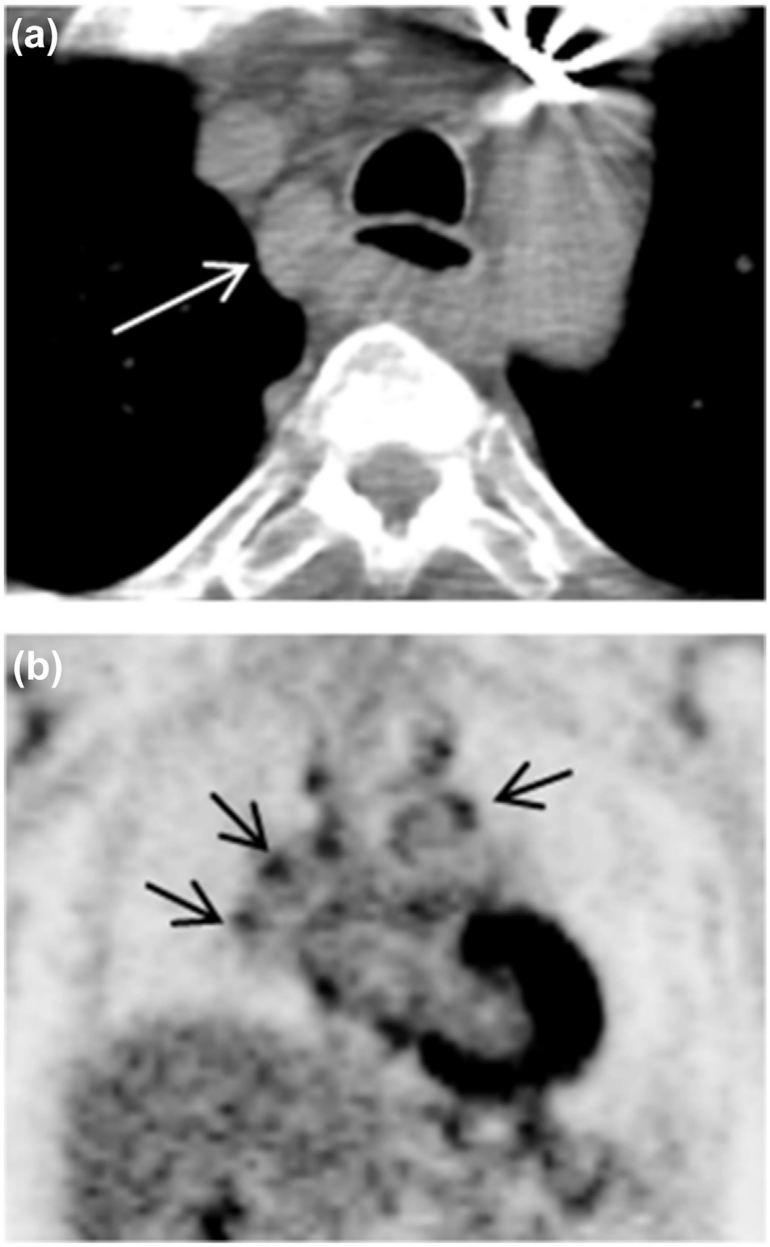

Fig. 3.

Axial CT image (a) revealed lymph node enlargement on 2R (arrow). Long-axis diameter is 2.38 cm, and short-axis diameter is 1.53 cm. The axial S/L ratio is 0.64. The lymph node had sharpness border. PET coronal image (b) show multiple mediastinal lymph nodes high FDG uptake (arrow). The pathology result is inflammation.

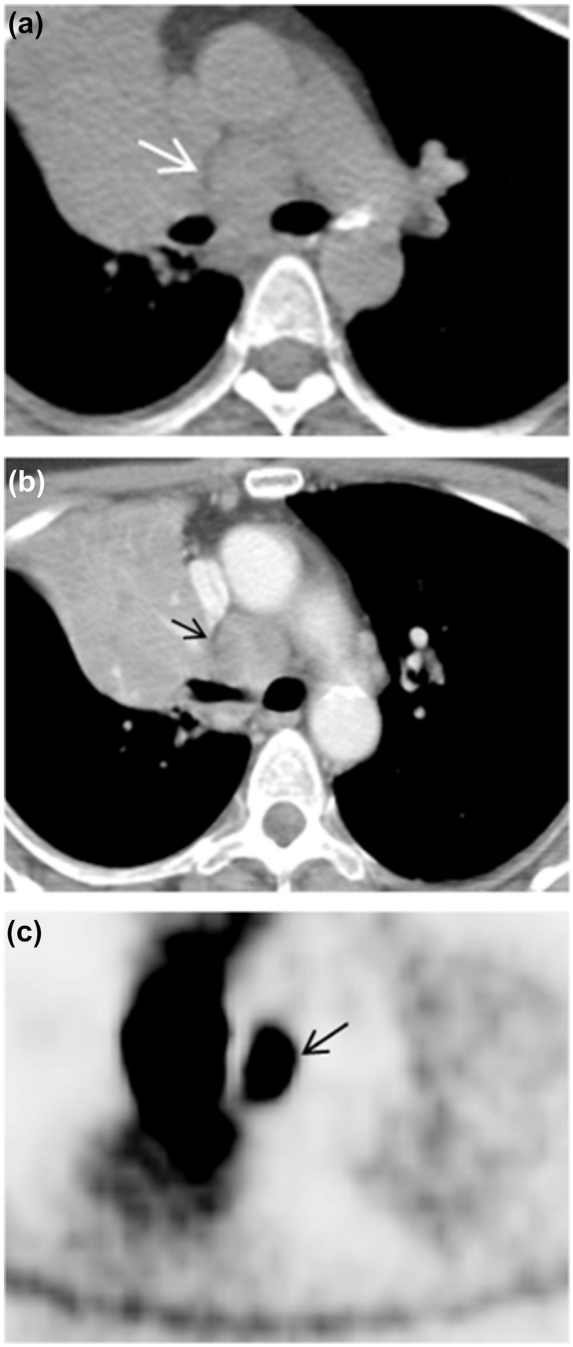

Fig. 4.

Axial CT image with (b) and without IV contrast (a) revealed lymph node enlargement on 4 (arrow). Long-axis diameter is 2.49 cm, and short-axis diameter is 2.36 cm. The axial S/L ratio is 0.95. Non-enhancement contrast CT value and enhancement contrast CT value were 42.52 and 90.21HU, respectively. The lymph node had un-sharpness border. Axial PET image (c) revealed the lymph node has high FDG uptake (arrow). The pathology result is B lymphoma.

Table 1

Location of LNs sampled by EBUS-TBNA.

Locations	Malignant LNs numbers	Inflammatory LNs numbers	Total n (%)
2L	2	0	2 (2/124, 1.61%)
2R	5	3	8 (8/124, 6.45%)
4L	7	6	13 (13/124, 10.48%)
4R	20	20	40 (40/124, 32.26%)
7	15	12	27 (27/124,21.77%)
10L	3	2	5 (5/124, 4.03%)
10R	8	6	14 (14/124, 11.29%)
11L	1	3	4 (4/124, 3.23%)
11R	3	8	11 (11/124, 8.87%)
Total	64	60	124 (124/124, 100%)

LN: lymph node; EBUS-TBNA: Endobronchial ultrasound guided transbronchial needle aspiration.

Table 2

Summary of cytological diagnoses of hilar and mediastinal lymph nodes.

Diagnosis	LNs number (%)
Lymphoma	18 (18/124, 14.52%)
NSCLC	27 (32/124, 25.81%)
Metastatic extra-thoracic Cancer	9 (9/124, 7.26%)
SCLC	8 (8/124, 6.45%)
Seminoma	2 (2/124, 1.61%)
Inflammatory reactive	48 (48/124, 38.71%)
Granuloma	12 (12/124, 9.68%)
Total LNs	124 (124/124, 100%)

LN: lymph node; NSCLC: non-small lung cancer; SCLC: small cell lung cancer.

Table 3

PET/CT continuous variables of inflammatory and malignant lymph nodes.

Parameters		Inflammation	Malignant	P value
Size	LAD	1.87 ± 0.64	2.38 ± 1.11	p = 0.002
	SAD	1.07 ± 0.38	2.03 ± 1.01	p < 0.001
	Axial S/L ratio	0.57 ± 0.09	0.85 ± 0.11	p < 0.001
CT HU	Non-enhancement CT value	33.07 ± 14.31	35.41 ± 9.78	p = 0.304

PET = positron emission tomography; CT = computed tomography.

LAD = long-axis diameter; SAD = short-axis diameter; Axial S/L ratio = short-axis diameter/long-axis diameter.

Continuous variables were analyzed using one-way ANOVA.

Table 4

The sensitivity, specificity, PPV, NPV, accuracy and DOR.

	SUV>2.5	SUV + SAD>1.0	SUV + Axial S/L ratio>0.7
Sensitivity	95.31% (61/64)	89.06% (57/64)	87.5% (56/64)
Specificity	20% (12/60)	53.33% (32/60)	93.33% (56/60)
PPV	55.96% (61/109)	67.06% (57/85)	93.33% (56/60)
NPV	80% (12/15)	82.05% (32/39)	87.5% (56/64)
Accuracy	58.87% (73/124)	71.77% (89/124)	90.32% (112/124)
DOR	5	9.31	98

PPV = positive predictive value; NPV = negative predictive value; SAD = short-axis diameter; Axial S/L ratio = short-axis diameter/long-axis diameter; DOR = Diagnostic odds ratio.